Journal of Alloys and Compounds 364 (2004) 29–36

Journal of ALLOYS AND COMPOUNDS

www.elsevier.com/locate/jallcom

Mössbauer effect studies of $Dy[(Fe_{0.7}Co_{0.3})_{1-x}Al_x]_2$ and $Dy[(Fe_{0.4}Co_{0.6})_{1-x}Al_x]_2$ compounds

J. Pszczoła [a,*], P. Stoch [a], J. Suwalski [b], J. Żukrowski [a]

[a] *Solid State Physics Department, Faculty of Physics and Nuclear Techniques, AGH, Al. Mickiewicza 30, 30-059 Kraków, Poland*
[b] *Institute of Atomic Energy, 05-400 Świerk-Otwock, Poland*

Received 8 August 2002; received in revised form 19 May 2003; accepted 19 May 2003

Abstract

^{161}Dy Mössbauer effect studies were performed for the $Dy[(Fe_{0.7}Co_{0.3})_{1-x}Al_x]_2$ and $Dy[(Fe_{0.4}Co_{0.6})_{1-x}Al_x]_2$ series (4.2 K) and the hyperfine interaction parameters were determined from the experimental Mössbauer spectra. It was found that, as a result of the ($Fe_{0.7}$ $Co_{0.3}$)/Al (first series) or ($Fe_{0.4}Co_{0.6}$)/Al (second series) substitution, the ^{161}Dy magnetic hyperfine fields decrease nonlinearly with the Al-content and form new branches of the ^{161}Dy Slater–Pauling dependence previously determined for the $Dy(M–M)_2$ series (M–M = Mn–Fe, Fe–Co, Co–Ni). Additionally, using the ^{57}Fe Mössbauer effect the magnetic ordering temperatures were obtained. The influence of Al-substitution, i.e., the reduction of the number of 3d-electrons, on the 3d-band and the 5d-band structure is qualitatively discussed.

Keywords: Rare earth compounds; Transition metal compounds; Hyperfine interactions; Mössbauer spectroscopy

1. Introduction

Heavy rare earth (R)-transition metal (M) compounds have been widely studied because of scientific and practical reasons [1–6]. The ferrimagnetism of these intermetallics is mainly driven by the 3d electrons [5].

The significance of the 3d-electrons was previously experimentally studied using the ^{57}Fe Mössbauer effect performed for the $Dy(M–M)_2$ (M–M = Mn–Fe, Fe–Co) intermetallic series [5,6]. The magnetic hyperfine field $\mu_0 H_{hf}$ (μ_0 is the magnetic permeability) observed at ^{57}Fe nuclei treated as a function of the average number n of 3d-electrons behaves according to the ^{57}Fe Slater–Pauling curve [5,6]. The maximum value of the field appears for the $Dy(Fe_{0.7}Co_{0.3})_2$ compound ($n = 6.3$). At this Co-content the filling up of the majority 3d-subband by 3d-electrons is terminated, whereas the minority 3d-subband is filled up only partially. Further Fe/Co substitution continues the filling-up of the minority subband and, for instance, for the compound $Dy(Fe_{0.4}Co_{0.6})_2$ this filling-up has progressed.

In order to test the 3d-electron significance, as a next step, the Al-substituted series $Dy[(Fe_{0.7}Co_{0.3})_{1-x}Al_x]_2$ and $Dy[(Fe_{0.4}Co_{0.6})_{1-x}Al_x]_2$ were studied using the ^{57}Fe Mössbauer effect. It was found that the magnetic hyperfine fields $\mu_0 H_{hf}(n)$ create new branches which bifurcate from the above mentioned ^{57}Fe Slater–Pauling curve [7,8].

In the present paper the substitution of Al into the M-sublattice in the $Dy[(Fe_{0.7}Co_{0.3})_{1-x}Al_x]_2$ and $Dy[(Fe_{0.4}Co_{0.6})_{1-x}Al_x]_2$ series was used to study the influence of the 3d-electrons on the magnetism of these R–M compounds and especially on the magnetism of their R-sublattice. For this purpose ^{161}Dy Mössbauer effect studies (4.2 K) were performed for both the series of intermetallics.

2. Intermetallics

The synthesis, X-ray studies and crystal structures of the intermetallic series $Dy[(Fe_{0.7}Co_{0.3})_{1-x}Al_x]_2$ and $Dy[(Fe_{0.4}Co_{0.6})_{1-x}Al_x]_2$ are described in Refs. [7,8]. It is worth to mention some crystallographic data. Namely, for the compounds with low Al-content, the cubic, *Fd3m*, $MgCu_2$-type (C15) Laves phases are observed. Further Al-substitution introduces crystallographic transitions, and for the intermediate Al-contents almost single phase compounds with the hexagonal *P6$_3$/mmc*, $MgZn_2$-type (C14) phase appear for both series. For the Al-rich side the

* Corresponding author.
E-mail address: pszczola@uci.agh.edu.pl (J. Pszczoła).

0925-8388/$ – see front matter © 2003 Elsevier B.V. All rights reserved.
doi:10.1016/S0925-8388(03)00549-8

compounds adopt again the crystallographic structure of the $MgCu_2$-type [7,8]. Both Laves phases, cubic and hexagonal, bear similarities and are described in detail elsewhere [9,10].

In the $MgCu_2$-type structure the unit cell contains 24 atoms, i.e., eight formula units of RM_2. The cubic phase has two non-equivalent crystallographic positions. The 8a sites are occupied by R-atoms (Mg-sites), whereas the M-atoms occupy the 16d positions (Cu-sites). Each rare earth ion (R) has 12 transition metal atoms (M) in the nearest neighbour shell (radius $a\sqrt{11}/8, a$ is the lattice constant) and four slightly more distant rare earth ions (R). The transition metal atoms occupy the 16d positions (Cu-sites). The transition metal atom is surrounded by six 3d-metal atoms as nearest-neighbours at distance $a\sqrt{2}/4$ and six R-ions (at $a\sqrt{11}/8$ as next-nearest-neighbours [9,10]).

The $MgZn_2$-type structure is more complex. The rare earth ions (Mg sites) occupy the 4f positions, whereas the M-atoms occupy the 2a and 6h positions (Zn_I, Zn_{II} sites). Each rare earth ion is surrounded by 12 almost equidistant transition metal atoms (M) in the first-neighbour shell and four almost equidistant rare earth ions in the next-nearest neighbour shell. The M-atoms (2a and 6h-Zn sites) have almost the same crystallographic surroundings with six M atoms and six R atoms [9,10]. It can be seen that the nearest neighbourhoods of the Mg-sites (R-atoms) in both crystal structures are quite similar to each other.

3. ^{161}Dy Mössbauer effect

3.1. Experiment

The ^{161}Dy Mössbauer effect measurements were performed using the 25.65 keV γ-rays emitted from a ^{161}Tb source and using the conventional transmission technique. The source, kept at room temperature, was moved in a constant acceleration mode using a high velocity spectrometer.

The source was obtained by neutron irradiation in a nuclear reactor (for 2 weeks with a flux 2×10^{14} n cm^{-2} s^{-1}) of about 30 mg of the $^{163}Dy_{0.5}{}^{160}Gd_{0.5}F_3$ starting material which was encapsulated in an aluminium container [11]. The isotopes Dy and Gd were 90% enriched. The ^{163}Dy and ^{160}Gd separated isotopes were used in order to increase the specific activity (^{160}Gd) of the source and to decrease Mössbauer self-absorption (^{163}Dy) [12]. The prepared source had an unsplit Mössbauer line at room temperature. It should be added that the halflife time of the source is only 165.6 h. The 25.65 keV γ-quanta useful for the Mössbauer effect were emitted as a result of the nuclear E1 electromagnetic transition between the excited state $5/2^-$ and the ground state $5/2^+$. The dysprosium nucleus in the excited state has a magnetic dipole moment of $\mu^* = 0.592\mu_N$, μ_N is the nuclear Bohr magneton, and the quadrupole moment equals $Q^* = 2.34$ barn. In the ground state these quantities are, respectively, equal to $\mu = -0.479$ μ_N and $Q = 2.35$ barn [13–17].

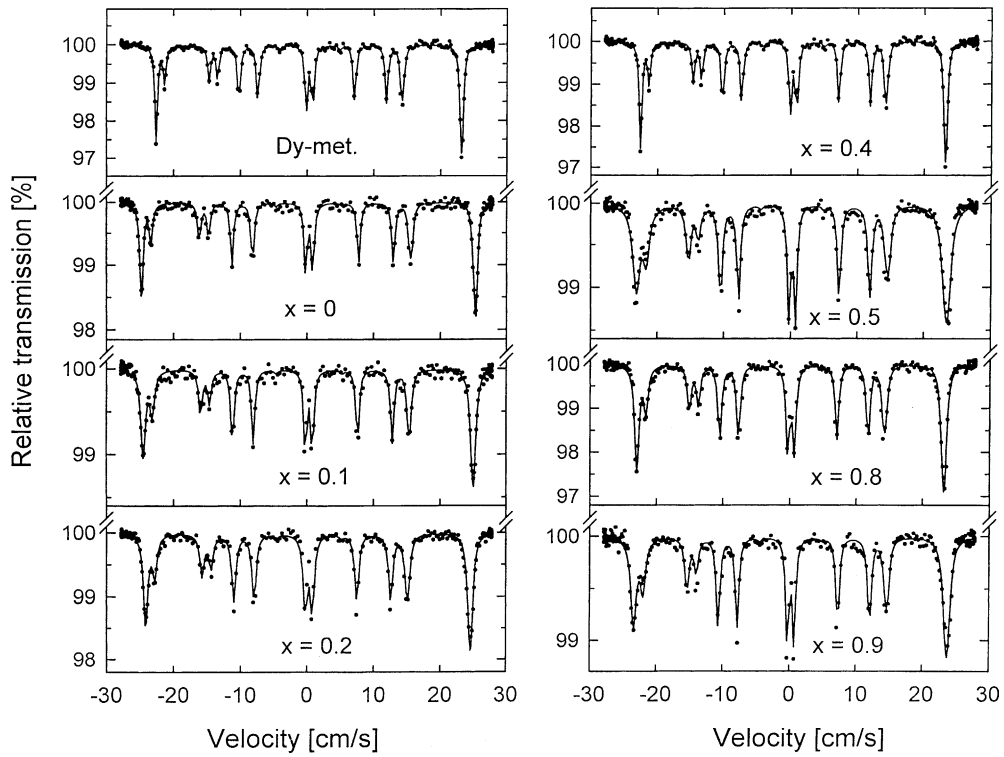

Fig. 1. The ^{161}Dy Mössbauer effect transmission spectra of the $Dy[(Fe_{0.7}Co_{0.3})_{1-x}Al_x]_2$ intermetallics (4.2 K). The spectrum for Dy-metal at 4.2 K has been used for calibration. Lines are fits.

The γ-quanta were detected by a krypton proportional counter. The counting gate was set over both the 25.65 keV peak and the escape peak around 12 keV.

It can be added that the $Dy[(Fe_{0.7}Co_{0.3})_{1-x}Al_x]_2$ and $Dy[(Fe_{0.4}Co_{0.6})_{1-x}Al_x]_2$ compounds were synthesised using dysprosium metal which was composed of natural abundance Dy isotopes (with 18.9% of ^{161}Dy). The polycrystalline absorbers in the form of discs were prepared from fine powder deposited on a thin aluminium foil with the use of shellac. For all the absorbers, the content of ^{161}Dy was about an optimal value equal to 8 mg/cm^2 [18].

3.2. The $Dy[(Fe_{0.7}Co_{0.3})_{1-x}Al_x]_2$ series

The resulting ^{161}Dy Mössbauer effect spectra (points) for Dy-metal and for the $Dy[(Fe_{0.7}Co_{0.3})_{1-x}Al_x]_2$ series collected at 4.2 K are presented in Fig. 1. The spectra were analysed using a least-squares fitting routine assuming one Zeeman pattern independent of the crystal structure, as described previously [19,20]. It can be understood considering that in the both crystal structures the rare earth ion is surrounded by similar neighbourhoods, as mentioned above. Moreover, it can be expected that a direct influence of the local randomness of the Fe/Co/Al nearest-neighbourhood on the hyperfine parameters of the Dy nuclei is presumably of secondary importance. Actually, the half-widths of the ^{161}Dy Mössbauer lines for the compounds (Table 1) are somewhat higher as compared to the half-width observed for Dy-metal. (The halfwidths are given in mm/s; 1 mm/s corresponds to 20.692(2) MHz [14].) It seems, that these differences could be related to an indirect influence, via 5d electrons, of the Fe/Co/Al neighbourhood of the Dy atoms, treated as averaged over the lattice during the fitting procedure. The fitted spectra (lines) follow satisfactorily the experimental points. The data obtained for Dy-metal were used for the calibration of the velocity scale of the spectrometer adopting the dysprosium metal parameters described in Refs [14,21].

Table 1 contains the isomer shifts IS, calculated in relation to a room temperature GdF_3 source [14,21], the hyperfine field parameter $g_N\mu_N H_{hf}h^{-1}$ and the electric quadrupole parameter $e^2qQ/4h$, where g_N is the nuclear Lande factor, H_{hf} is the hyperfine field, h is the Planck constant, q is the electric field gradient at the ^{161}Dy nuclei, e is the electron charge [15,19]. The obtained parameters versus x are shown in Fig. 2 [22].

Table 1
The hyperfine interaction parameters observed at ^{161}Dy nuclei in the intermetallics (at 4.2 K)

Compound	IS/h [MHz]	$g_N\mu_N H_{hf}/h$ [MHz] $\mu_0 H_{hf}$ (T)	$e^2qQ/(4h)$ [MHz]	$\Gamma/2$ (mm/s)
$Dy[(Fe_{0.7}Co_{0.3})_{1-x}Al_x]_2$				
Dy-met.	84.0(3.0)	835.1(1.5) 580.3(2.3)	655(2)	2.60(5)
$Dy(Fe_{0.7}Co_{0.3})_2$	81.93(5.0)	914.5(3.0) 635.5(2.0)	713(2)	2.82(7)
$Dy[(Fe_{0.7}Co_{0.3})_{0.9}Al_{0.1}]_2$	78.41(6.0)	904.6(3.0) 628.6(2.0)	713(6)	2.83(7)
$Dy[(Fe_{0.7}Co_{0.3})_{0.8}Al_{0.2}]_2$	73.86(4.0)	890.6(1.0) 618.9(1.0)	699(2)	3.77(6)
$Dy[(Fe_{0.7}Co_{0.3})_{0.6}Al_{0.4}]_2$	66.41(6.0)	860.3(3.0) 597.8(2.0)	658(4)	2.96(7)
$Dy[(Fe_{0.7}Co_{0.3})_{0.5}Al_{0.5}]_2$	67.86(6.0)	851.6(3.0) 591.8(2.0)	632(2)	2.94(6)
$Dy[(Fe_{0.7}Co_{0.3})_{0.2}Al_{0.8}]_2$	56.48(6.0)	842.7(3.0) 585.6(2.0)	624(4)	3.59(8)
$Dy[(Fe_{0.7}Co_{0.3})_{0.1}Al_{0.9}]_2$	49.86(4.0)	842.7(1.0) 585.6(1.0)	645(2)	3.28(5)
$DyAl_2$ [23]	–	– 582(2.0)	–	–
$Dy[(Fe_{0.4}Co_{0.6})_{1-x}Al_x]_2$				
$Dy(Fe_{0.4}Co_{0.6})_2$	78.41(1.0)	894.1(1.0) 621.3(1.0)	709(2)	3.25(7)
$Dy[(Fe_{0.4}Co_{0.6})_{0.9}Al_{0.1}]_2$	75.30(1.0)	888.3(3.0) 617.3(2.0)	700(6)	3.78(8)
$Dy[(Fe_{0.4}Co_{0.6})_{0.8}Al_{0.2}]_2$	69.30(2.0)	875.7(6.0) 608.5(4.0)	679(8)	4.1(1)
$Dy[(Fe_{0.4}Co_{0.6})_{0.6}Al_{0.4}]_2$	70.75(1.0)	852.2(3.0) 592.2(2.0)	641(4)	4.2(1)
$Dy[(Fe_{0.4}Co_{0.6})_{0.5}Al_{0.5}]_2$	62.89(1.0)	846.8(3.0) 588.4(2.0)	625(2)	3.75(7)

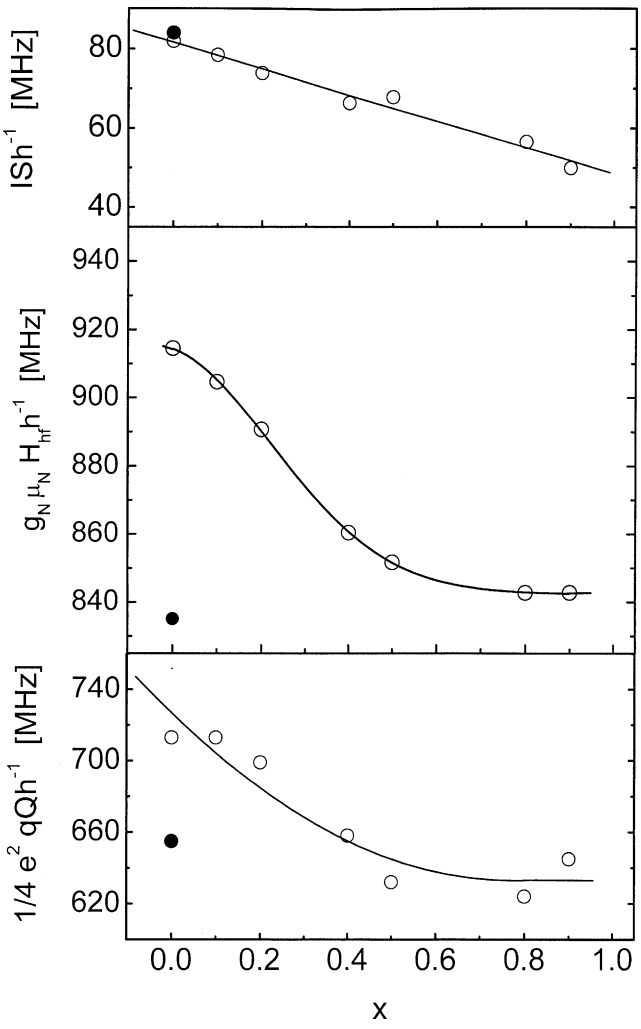

Fig. 2. The ^{161}Dy hyperfine interaction parameters of the Dy[$(Fe_{0.7}Co_{0.3})_{1-x}Al_x]_2$ series (4.2 K): the isomer shift (IS), the magnetic hyperfine field H_{hf} and the electric field gradient q. The parameters for Dy-metal (4.2 K) added (black points). Lines are polynomial fits. Preliminary data presented at All-Polish Seminar on Mössbauer Spectroscopy, Radom-Zbożenna, 12–14 June 2000 [22].

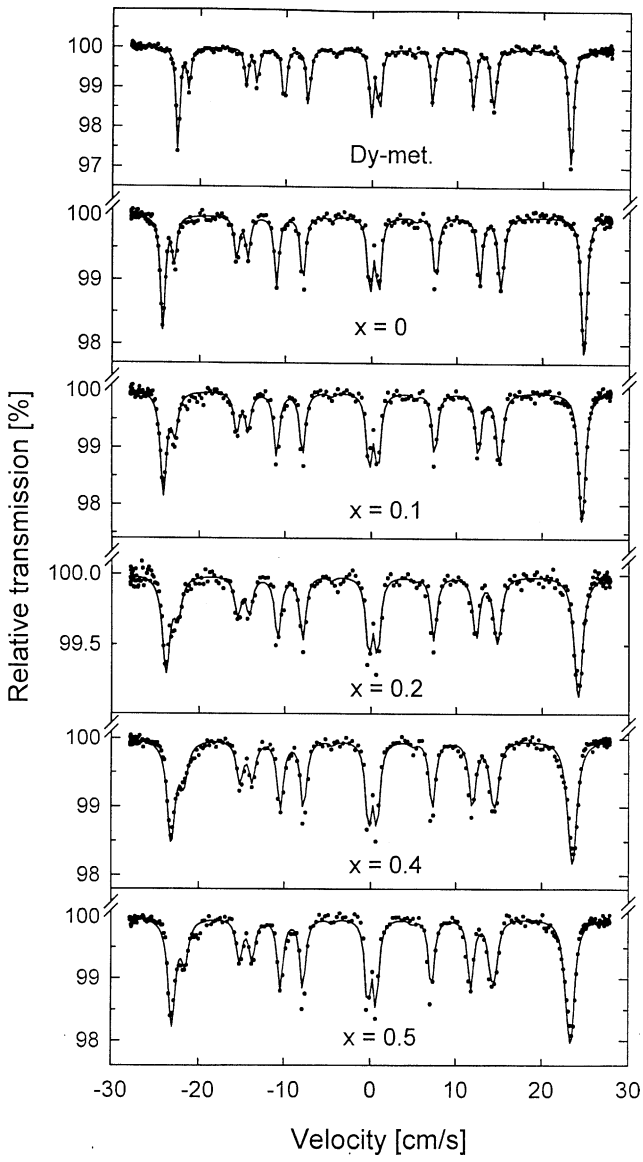

Fig. 3. The ^{161}Dy Mössbauer effect transmission spectra of the Dy[$(Fe_{0.4}Co_{0.6})_{1-x}Al_x]_2$ intermetallics (4.2 K). The spectrum for Dy-metal at 4.2 K has been used for calibration. Lines are fits.

3.3. The Dy[$(Fe_{0.4}Co_{0.6})_{1-x}Al_x]_2$ series

The experimental ^{161}Dy Mössbauer spectra (points) for Dy-metal and for the Dy[$(Fe_{0.4}Co_{0.6})_{1-x}Al_x]_2$ series measured at 4.2 K are presented in Fig. 3. An analogous fitting procedure (as described above) was used and the obtained hyperfine parameters versus x are shown in Fig. 4.

3.4. Dependencies of parameters

The hyperfine interaction parameters for both series change to some extent analogously versus x. Namely, the isomer shifts IS(x) observed at the ^{161}Dy nuclei decrease approximately linearly with the Al-content x. The previously obtained isomer shifts at the ^{57}Fe nuclei, for both the series, increase with x [7,8]. These opposite tendencies were already qualitatively discussed for another Al-substituted series [19]. Here it is worth to mention that as a result of the Al-dilution of the transition metal sublattice, the itinerancy of both the 3d-electrons and the 5d-electrons is reduced. Consequently the 3d electron density at Fe atoms and the 5d electron density at Dy atoms increase, introducing the observed changes for both isomer shifts, as discussed elsewhere [19,23,24].

Similarly, the electric field gradients at the dysprosium nuclei for both series decrease with x (Figs. 2 and 4). The electric field gradients observed at dysprosium nuclei (and more generally at rare earth nuclei) in rare earth transition metal compounds were discussed previously in the literature [15,20,24]. Namely, the electric field gradient at the ^{161}Dy nuclei can be treated as a sum of the electric field gradient q_{4f}, which arises from the 4f shell, and the lattice

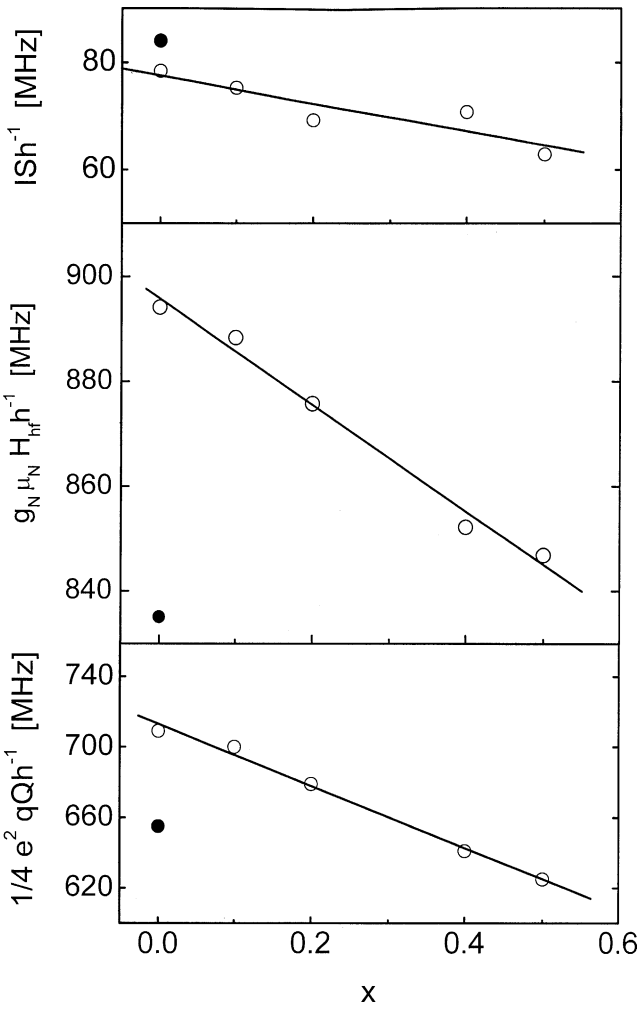

Fig. 4. The ^{161}Dy hyperfine interaction parameters of the Dy[$(Fe_{0.4}Co_{0.6})_{1-x}Al_x]_2$ series (4.2 K): the isomer shift IS, the magnetic hyperfine field H_{hf} and the electric field gradient q. The parameters for Dy-metal (4.2 K) are added (black points). Lines are fits, to follow experimental points.

contribution q_l. Assuming that there is magnetic saturation at 4.2 K, so that for the Dy^{3+} ions the quantum number $J_z = J = 15/2$ can be assumed. In that case the q_{4f} contribution should be constant across the series. Therefore it can be expected that the changes in the electric field gradient approximately can be ascribed to the lattice contribution.

The hyperfine fields $H_{hf}(x)$ considerably decrease with x for both the series. It can be mentioned that the hyperfine fields in the magnetically saturated R–M intermetallics adopt higher values as compared to the free Dy^{3+}-ion value [24]. It can be added that the field observed for dysprosium metal at 4.2 K (835 MHz [14,15]) is somewhat higher than the field known for the free ion. The hyperfine field observed at the rare earth nuclei in the intermetallics can be treated as a sum of the field H_{4f} created by the well localized 4f electrons, the H_{sp}-contribution caused by the polarization of the neighbouring conduction electrons originating from the parent 4f-shell, the H_{tR}-contribution caused by the neighbouring and more distant rare earth moments and the H_{tM}-contribution caused by the transition metal moments [20,24].

As the core of the rare earth atom is well shielded from the rest of the crystal lattice by the outer valence electrons a considerable direct influence of the transition metal atoms on the hyperfine field at the ^{161}Dy nucleus is absent [5,6]. The band-type 5d electrons are partly localized on their parent ions [25], thus the field H_{tM} is produced by the 5d(6s) electrons which actually are polarized by the surrounding transition metal atoms.

The sum of the last three terms is called the excess hyperfine field [20,23]. In practice, following the experimental H_{hf} values, the excess hyperfine field can be calculated using the approximate expression $\Delta H_{hf} = H_{hf} - H_{4f}$. The field H_{4f} can satisfactorily be approximated by the hyperfine field observed in Dy metal [20,24]. In the heavy rare earth-transition metal compounds, the field H_{4f} can be treated as being constant across the series. It is known that the contribution $|\mathbf{H}_{sp} + \mathbf{H}_{tR}|$ does not have too big a value [20,24]. Considering the above facts, the excess value can be approximated by: $\Delta H_{hf}(n) \cong H_{tM}(n)$. Thus the excess hyperfine field should be sensitive to the average to composition and the magnetic changes in the transition metal sublattice. Therefore, the dependence of the total hyperfine field on the aluminium content x can be ascribed to the change in excess hyperfine field.

It was already discussed that there is no proportionality between the magnetic moment of the 3d electrons and the excess ^{161}Dy hyperfine field [5]. The excess ^{161}Dy hyperfine field should be related to the induced magnetization of the 5d-band.

4. The ^{161}Dy Slater–Pauling curve and branches

Fig. 5 (curve 1) shows, given for a comparison, the previously reported ^{161}Dy hyperfine fields $\mu_0 H_{hf}(n)$ for the $Dy(Mn_{1-x}Fe_x)_2$, $Dy(Fe_{1-x}Co_x)_2$ and $Dy(Co_{1-x}Ni_x)_2$ series (at 4.2 K) plotted versus the average number n of 3d electrons calculated per transition metal atom [5]. The field $\mu_0 H_{hf}(n)$ strongly depends on the number n and creates the ^{161}Dy Slater–Pauling curve with a maximum at about $n = 5.9$ [5].

Fig. 5 (curve 2) presents the new branch of the ^{161}Dy Slater–Pauling curve obtained for the Dy[$(Fe_{0.7}Co_{0.3})_{1-x}Al_x]_2$ series. Two somewhat different experimental points for $n = 6.3$ correspond to different measurements, but they are close together within the frame of experimental errors. It should be added that in this case the hyperfine field depends on the average number n of 3d electrons, formally calculated per one site of the transition metal sublattice, using the formula $n = (0.7 \times 6 + 0.3 \times 7)(1 - x)$, where 6 and 7 are the numbers of 3d electrons at the Fe, Co atoms, respectively.

Analogously, Fig. 5 (curve 3) presents the new branch of the ^{161}Dy Slater–Pauling curve obtained for the

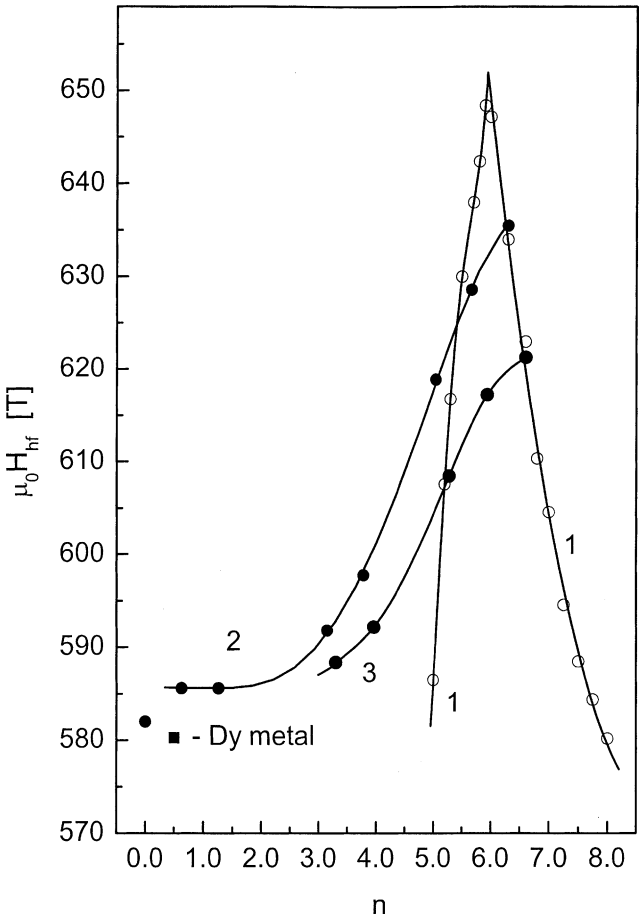

Fig. 5. The Slater–Pauling curves: (1) the ^{161}Dy magnetic hyperfine field $\mu_0 H_{hf}(n)$ for Dy(M–M)$_2$ series (M–M = Mn–Fe, Fe–Co, Co–Ni), (4.2 K); (2) the ^{161}Dy branch $\mu_0 H_{hf}(n)$ for the Dy[(Fe$_{0.7}$Co$_{0.3}$)$_{1-x}$Al$_x$]$_2$ series (4.2 K); (3) the ^{161}Dy branch $\mu_0 H_{hf}(n)$ for the Dy[(Fe$_{0.4}$Co$_{0.6}$)$_{1-x}$Al$_x$]$_2$ series (4.2 K). DyAl$_2$ value ($n = 0$) [23] and Dy-metal value are added. Lines are polynomial fits.

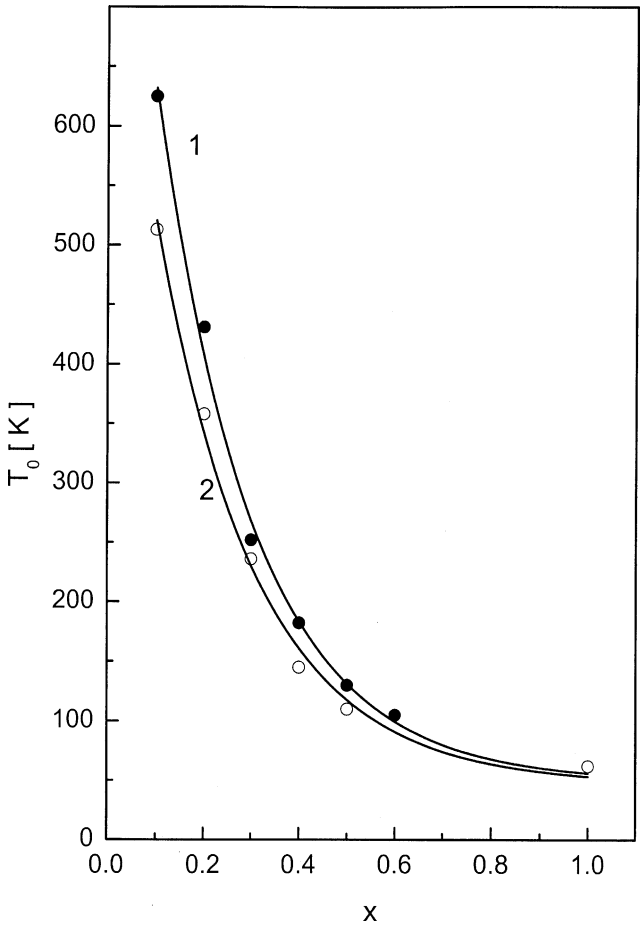

Fig. 6. The magnetic ordering temperatures for the Dy[(Fe$_{0.7}$Co$_{0.3}$)$_{1-x}$Al$_x$]$_2$ (1), and Dy[(Fe$_{0.4}$Co$_{0.6}$)$_{1-x}$Al$_x$]$_2$ (2) series. Lines are exponential fits.

Dy[(Fe$_{0.4}$Co$_{0.6}$)$_{1-x}$Al$_x$]$_2$ series. In this case $n = (0.4 \times 6 + 0.6 \times 7)(1-x)$.

For both the series the hyperfine fields $\mu_0 H_{hf}(n)$ do not decrease linearly with n, but it should be emphasized that there are no maxima for these curves. It means that for the ^{161}Dy nuclei as well as for the ^{57}Fe nuclei there is no Slater–Pauling behaviour in the Al-substituted series [7,8].

5. Curie temperatures

The magnetic ordering temperatures of the Dy[(Fe$_{0.7}$Co$_{0.3}$)$_{1-x}$Al$_x$]$_2$ and the Dy[(Fe$_{0.4}$Co$_{0.6}$)$_{1-x}$Al$_x$]$_2$ series were determined with an approximate accuracy of $\Delta T = 5$ K using the temperature dependence of the ^{57}Fe Mössbauer spectra (not presented). The method was described elsewhere [26,27]. The Curie temperatures for both the series as functions of the aluminium contribution x are presented in Fig. 6.

The ordering temperatures for the Dy[(Fe$_{0.7}$Co$_{0.3}$)$_{1-x}$ Al$_x$]$_2$ series are equal to 625, 431, 252, 182, 130, 105 and 62 K [1] for $x = 0.1$, 0.2, 0.3, 0.4, 0.5, 0.6 and 1.0, respectively. Analogously, the ordering temperatures for the Dy[(Fe$_{0.4}$Co$_{0.6}$)$_{1-x}$Al$_x$]$_2$ series are equal to 513, 358, 236, 145, 110 and 62 K for $x = 0.1$, 0.2, 0.3, 0.4, 0.5 and 1.0, respectively. For each series the ordering temperature is strongly nonlinearly reduced with x.

6. Discussion

The influences of the Al-substitution in the Dy[(Fe$_{0.7}$Co$_{0.3}$)$_{1-x}$Al$_x$]$_2$ and Dy[(Fe$_{0.4}$Co$_{0.6}$)$_{1-x}$Al$_x$]$_2$ series on the crystal structure, on the hyperfine interactions at the ^{57}Fe nuclei, especially on the ^{57}Fe hyperfine field were discussed elsewhere [7,8].

In order to discuss the obtained ^{161}Dy data it is useful to relate these results to the known ^{57}Fe data. Fig. 7 contains the ^{161}Dy Slater–Pauling curve (1) known for Dy(M–M)$_2$ (M–M = Mn–Fe, Fe–Co, Co–Ni) [5] with branch (2) obtained for Dy[(Fe$_{0.7}$Co$_{0.3}$)$_{1-x}$Al$_x$]$_2$ and (3) for Dy[(Fe$_{0.4}$Co$_{0.6}$)$_{1-x}$Al$_x$]$_2$. These are compared to the ^{57}Fe Slater–Pauling curve (4) for Dy(M–M)$_2$ (M–M = Mn–Fe,

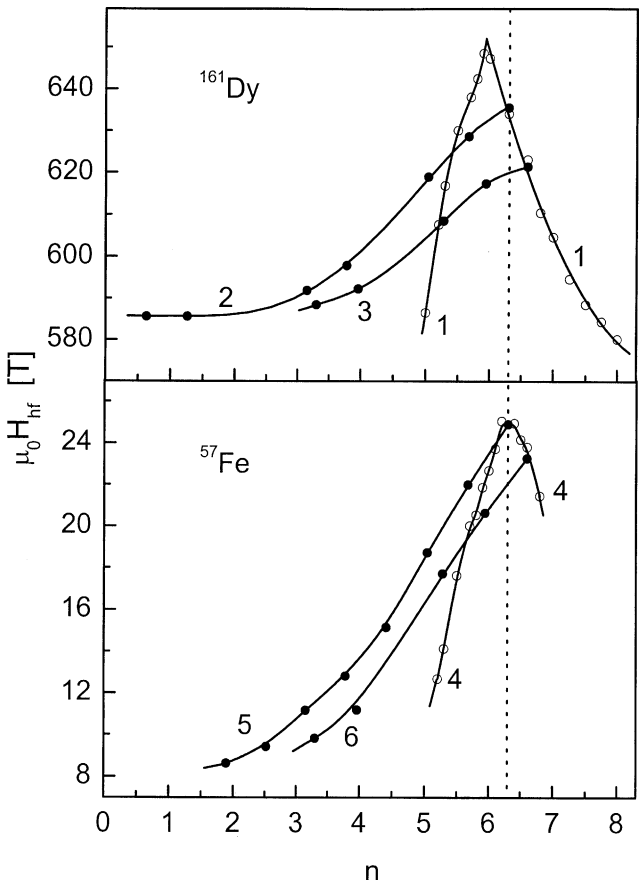

Fig. 7. The ^{161}Dy Slater–Pauling curve (1) for Dy(M–M)$_2$ (M–M = Mn–Fe, Fe–Co, Co–Ni) with branch (2) for Dy[(Fe$_{0.7}$Co$_{0.3}$)$_{1-x}$Al$_x$]$_2$ and (3) for Dy[(Fe$_{0.4}$Co$_{0.6}$)$_{1-x}$Al$_x$]$_2$ compared to the ^{57}Fe Slater–Pauling curve (4) for Dy(M–M)$_2$ (M–M = Mn–Fe, Fe–Co) with branch (5) for Dy[(Fe$_{0.7}$Co$_{0.3}$)$_{1-x}$Al$_x$]$_2$ and (6) for Dy[(Fe$_{0.4}$Co$_{0.6}$)$_{1-x}$Al$_x$]$_2$.

Fe–Co) [5,6], branch (5) for Dy[(Fe$_{0.7}$Co$_{0.3}$)$_{1-x}$Al$_x$]$_2$ [7] and branch (6) for Dy[(Fe$_{0.4}$Co$_{0.6}$)$_{1-x}$Al$_x$]$_2$ [8]. The observed ^{161}Dy hyperfine fields, in the Al-substituted series, decrease to some extent analogously against the number n as the ^{57}Fe hyperfine fields of their counterparts.

The reduction of the ^{57}Fe hyperfine field was related to changes in the 3d-band. It was already discuss that the Al-dilution reduces the number u_{M-M} of the transition metal nearest neighbours surrounding a given Fe-atom, the 3d–3d exchange interactions are weakened step by step with x and there is an increase of the mean 3d atom–3d atom distance. As a result the overlap among the 3d wave functions of the neighbouring atoms is reduced and consequently the 3d electrons become more localized [28]. The energy shift [29,30] between the 3d subbands $\Delta E_{3d} = J_{3d-3d} u_{M-M} m_M$ is reduced (J_{3d-3d} is the exchange integral between 3d electrons) and as a result the 3d-electrons are redistributed over the 3d-subbands. Consequently, the magnetic moment m_M per 3d-atom and the hyperfine field H_{hf} at the iron atom, the contribution from the transition metal sublattice to the ordering temperature and thus the ordering temperature T_o are reduced step by step across the series [7,8].

Considering the previously introduced idea that the excess hyperfine field is created by the 5d-band, actually polarized by the 3d-band, it can be expected that the 5d-band changes to some extent analogously to the 3d-band. The excess hyperfine field at the ^{161}Dy nuclei is induced by the transition metal sublattice via the 5d6s electrons [5].

The Al-substitution reduces the average number u_{R-M} of the transition metal nearest neighbours surrounding a given Dy-atom and thus reduces the energy shift $\Delta E_{5d-3d} \cong J_{5d-3d} u_{R-M} m_M$ [29,30] between the 5d subbands, where J_{5d-3d} is the average exchange integral for 5d and 3d electrons. Consequently the 5d electrons should also become gradually redistributed over the 5d-subbands and the difference between the majority and minority 5d electron densities should become reduced step by step with x. Therefore the magnetic moment m_{5d} per rare earth atom and thus the excess hyperfine field should also decrease and lead finally to the ^{161}Dy branch of the Slater–Pauling curve induced by the Al, i.e., by the 3d4s/3sp electron substitution [5]. Since both the numbers u_{M-M} and u_{R-M} decrease proportionally to the Al-content x, a certain analogy in the change between the $\mu_0 H_{hf}(^{57}\text{Fe};n)$ and $\mu_0 H_{hf}(^{161}\text{Dy};n)$ in the Al-substituted series is observed.

The above approach, using rigid band model ideas, seems to be satisfactory enough for this qualitative level discussion. For a more sound discussion further experimental, theoretical and numerical studies would be useful.

Acknowledgements

Supported partially by Polish Committee of Scientific Studies, grant no. 2PO 3B 166 14. M. Mróz and J. Ozimkowski are acknowledged for technical assistance.

References

[1] K.N.R. Taylor, Adv. Phys. 20 (1971) 551.
[2] K.H.J. Buschow, in: E.P. Wohlfarth (Ed.), Ferromagnetic Materials, Vol. 1, North Holland, Amsterdam, 1980.
[3] E. Burzo, H.R. Kirchmayr, in: K.A. Gschneidner, L. Eyring (Eds.), Handbook on the Physics and Chemistry of Rare Earths, Vol. 12, North Holland, Amsterdam, 1989.
[4] I.A. Campbell, J. Phys. F: Metal Phys. 2 (1972) L47.
[5] B. Gicala, J. Pszczoła, Z. Kucharski, J. Suwalski, Phys. Lett. A185 (1994) 491.
[6] B. Gicala, J. Pszczoła, Z. Kucharski, J. Suwalski, Solid State Commun. 96 (1995) 511.
[7] J. Pszczoła, A. Feret, B. Winiarska, L. Dąbrowski, J. Suwalski, J. Alloys Comp. 299 (2000) 59.
[8] J. Pszczoła, B. Winiarska, Z. Kucharski, J. Suwalski, J. Alloys Comp. 265 (1998) 15.
[9] F. Laves, Naturwissenschaften 27 (1939) 65.
[10] J. Chojnacki, Structural Metallography, Śląsk Press, Katowice, 1966, (in Polish).
[11] S. Ofer, I. Nowik, S. Cohen, in: V.I. Goldanskij (Ed.), Chemical Applications of Mössbauer Spectroscopy, Vol. 27, Academic Press, New York, 1968.

[12] R.L. Cohen, H.J. Guddenheim, Nucl. Instrum. Methods 71 (1969) 27.
[13] N.N. Greenwood, T.C. Gibb, in: Mössbauer Spectroscopy, Chapman, London, 1971.
[14] J.G. Stevens, B.D. Dunlop, J. Phys. Chem. Ref. Data 5 (1976) 1093.
[15] H.P. Wit, L. Niesen, H. de Waard, Hyp. Int. 5 (1978) 233.
[16] J. Chappert, L. Asch, M. Boge, G.M. Kalvius, B. Boucher, J. Magn. Magn. Mater. 28 (1982) 124.
[17] M. Belakhovsky, J. Chappert, D. Schmidt, J. Phys. C: Solid State Phys. 10 (1977) L493.
[18] J. Piekoszewski, K. Kisyńska, L. Dąbrowski, Nukleonika 20 (1975) 947.
[19] J. Pszczoła, J. Żukrowski, J. Suwalski, J. Kucharski, M. Łukasiak, J. Magn. Magn. Mater. 40 (1983) 197.
[20] J. Pszczoła, J. Żukrowski, K. Krop, J. Suwalski, J. Magn. Magn. Mater. 44 (1984) 223.
[21] G.J. Bowden, R.K. Day, M. Sarwar, in: Intern. Conf. Magnetism, Vol. 4, Nauka, Moscow, 1974.
[22] J. Pszczoła, J. Suwalski, Mol. Phys. Rep. 30 (2000) 113.
[23] H. Maletta, G. Crecelius, W. Zinn, J. Phys. Suppl. 35 (1974) C-6-279.
[24] B. Bleaney, in: R.J. Elliot (Ed.), Magnetic Properties of Rare-Earth Metals, Plenum, London, 1972.
[25] B.N. Harmon, A.J. Freeman, Phys. Rev. B10 (1974) 1979.
[26] A.R. Chowdhury, G.S. Collins, C. Hohenemser, Hyp. Inter. 15/16 (1983) 617.
[27] M.A. Kobeissi, C. Hohenemser, Hyp. Inter. 4 (1978) 480.
[28] K.H.J. Buschow, J. Less-Common Metals 43 (1975) 55.
[29] W. Vonsovskij, in: Magnetizm, Nauka, Moscow, 1971 (in Russian).
[30] A.H. Morrish, in: The Physical Principles of Magnetism, 1st Edition, Wiley, New York, 1965.